

# Identification of hydrodynamic coefficients in ship maneuvering equations of motion by Estimation-Before-Modeling technique

Hyeon Kyu Yoon<sup>\*</sup>, Key Pyo Rhee

*Department of Naval Architecture and Ocean Engineering, Seoul National University, Shilim-dong,  
Kwanak-gu, Seoul 151-742, South Korea*

Received 2 December 2002; accepted 5 March 2003

---

## Abstract

Estimation-Before-Modeling (EBM) technique (or the two-step method) is a system identification method that estimates parameters in a dynamic model. Given sea trial data, the extended Kalman filter and modified Bryson–Frazier smoother can be used to estimate motion variables, hydrodynamic force, and the speed and the direction of current. And using these estimated data, we can use the ridge regression method to estimate the hydrodynamic coefficients in a model. An identifiable state space model is constructed in case that current effect is included and the maneuvering characteristics of a ship are analyzed by correlation analysis. To better identify hydrodynamic coefficients, we suggest the sub-optimal input scenario that considers the D-optimal criterion. Finally, the algorithm is confirmed against real sea trial data of 113K tanker.

© 2003 Elsevier Ltd. All rights reserved.

*Keywords:* Hydrodynamic coefficient; Estimation-Before-Modeling technique; Sea trial; Input scenario

---

## 1. Introduction

To analyze the maneuvering performance of a ship and design an autopilot, we must develop a mathematical model that can precisely describe the ship's motion. There has been much research on building a more accurate model describing the

---

<sup>\*</sup> Corresponding author. Tel.: +82-2-880-7339; fax: +82-2-887-6013.  
E-mail address: [hkyoon@kriso.re.kr](mailto:hkyoon@kriso.re.kr) (H.K. Yoon).

### Nomenclature

$\rho$	water density
$m$	ship's mass
$I_z$	ship's mass moment of inertia about $z$ -axis
$x_{G_b}$	$x_b$ coordinate of center of gravity of a ship
$S$	ship's wetted surface area
$u, v, r$	surge and sway velocities and heading angle rate with respect to the body-fixed frame
$u_r, v_r$	surge and sway velocity relative to current velocities
$U$	total speed of a ship
$X, Y, N$	surge and sway hydrodynamic forces and yaw hydrodynamic moment except the components due to added mass
$C_R$	resistance coefficient
$\eta_1, \eta_2, \eta_3$	thrust related coefficients
$n$	propeller rps
$\delta, e$	actual and effective rudder deflection angle
$c, c_0$	inflow speed at rudder position during maneuvering and straight running
$U_c$	constant speed of current
$\psi_c$	constant direction of current
$\psi_{c_r}$	relative heading angle with respect to current direction ( $= \psi - \psi_c$ )
$c_x, c_y$	$x, y$ components of the speed of current ( $= U_c \cos \psi_c, U_c \sin \psi_c$ )
$\eta'_{C_R}$	$= \eta'_1 - C_R S / L^2$
$D(t_k)$	$= H(\hat{x}(t_k t_{k-1}), t_k) P(t_k t_{k-1}) H^T(\hat{x}(t_k t_{k-1}), t_k) + R(t_k)$
$x_{D_b}, y_{D_b}$	$x_b, y_b$ coordinates of DGPS antenna
$X'_{vv}, X'_{vr}, \dots$	surge nondimensionalized hydrodynamic coefficients
$Y'_v, Y'_r, \dots$	sway nondimensionalized hydrodynamic coefficients
$N'_v, N'_r, \dots$	yaw nondimensionalized hydrodynamic coefficients

hydrodynamic force acting on a ship during maneuvers and obtaining hydrodynamic coefficients in it.

Two classes of hydrodynamic force model have been proposed by Abkowitz (Lewis, 1989) and MMG (Kobayashi et al., 1995). Abkowitz assumed that hydrodynamic force can be described by multiple polynomial equations of variables related to maneuvering motion, propeller rpm, and rudder angle consulting Taylor series expansion from a nominal condition. The hydrodynamic coefficient is obtained from the partial derivative of hydrodynamic force with respect to each variable. In the MMG model, hydrodynamic force is composed of three components namely the bare hull, propeller, and rudder force components which are determined by their respective source. And then, the model considers their interaction effects.

Hydrodynamic coefficients are obtained by various methods such as the captive model test, slender body theory, empirical formulae, computational fluid dynamics (CFD), system identification (SI), etc. Among them the planar motion mechanism (PMM) test, a type of the captive model test, is widely used because most coefficients can be obtained. But the scaling effect due to the inconsistency of the Reynold's number between the real ship and the scaled model still remains. SI has been applied to ship maneuvering and resistance problems to avoid the scaling effect by Källström (1979), Abkowitz (1980), Hwang (1980), and Liu (1988). Hwang (1980) dealt with hydrodynamic coefficients as augmented state variables to be obtained adopting the extended Kalman filter (EKF) technique. When the coefficients are augmented in the original state variable vector, the size of state error covariance matrix increases to the extent that it negatively effects the performance of estimation and the Jacobian matrix of the state equation becomes complex with increasing complexity of hydrodynamic force model.

Estimation-Before-Modeling (EBM) technique, so called the two-step method, has been applied to estimate the parameters in the aerodynamic model, which can describe the high angle of attack motion of an airplane as described by Sri-Jayantha and Stengel (1988), Hoff (1995) and Hoff and Cook (1996). Aerodynamic force is estimated at first by EKF and modified Bryson–Frazier (MBF) smoother, and then the aerodynamic coefficients are identified by regression analysis.

In this study, we first introduce the EBM technique to the ship maneuvering problem. State space model is constructed by selecting the appropriate motion variables such that the variables as well as the speed and the direction of current should be observable within the limits of the number of measurements in a ship's sea trial. As shown in Fig. 1, at first, the motion variables, hydrodynamic force, and the speed and the direction of current are estimated (Yoon and Rhee, 2001). In the second step, the hydrodynamic coefficients in the modified Abkowitz's model by Hwang (1980) are identified by ridge regression method. The main advantages of applying this technique to our problem are that the number of states to be estimated is small in comparison with that of the foregoing EKF technique, and the characteristics of the structure of hydrodynamic model can easily be analyzed as treating it to a multiple linear regression model. The specific characteristics of the problem such as the simultaneous drift phenomenon (Hwang, 1980) or the multicollinearity which make it difficult to identify each hydrodynamic coefficient separately, are confirmed by correlation analysis of motion variables. To resolve the multicollinearity problem in terms of D-optimal input criterion, we assess the

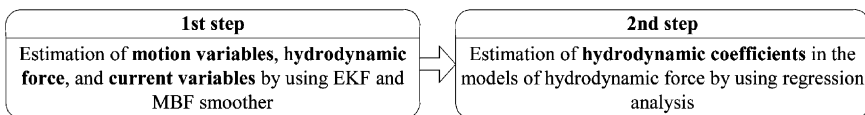


Fig. 1. Block diagram of EBM technique.

performance of estimation as a function of the maximum rudder angle and the period of the rudder command of pseudo random binary sequence (PRBS), and suggest sub-optimal input scenario. If a ship can respond sufficiently to the input scenario, multicollinearity in a regression model diminishes considerably.

We developed an algorithm for identifying hydrodynamic coefficients with the simulated data for 278K tanker named as ESSO OSAKA (Crane, 1979), which is the standard ship for the maneuvering committee of the International Towing Tank Conference (ITTC). Finally, the algorithm was validated against real sea trial data for the 113K tanker.

## 2. Construction of state space model

### 2.1. Maneuvering equations of motion including current effect

To describe a ship's maneuver, we introduced the three coordinate systems; the earth-fixed frame ( $O - xy$ ), the moving frame that moves at the speed of current ( $O_r - x_r y_r$ ), and the body-fixed frame ( $o - x_b y_b$ ) shown in Fig. 2. The earth-fixed frame is regarded as a space-fixed inertial frame, and its origin and direction are the same as those of the body-fixed frame at initial time of maneuver. The moving frame shares most of the earth-fixed frame except that the former moves at the

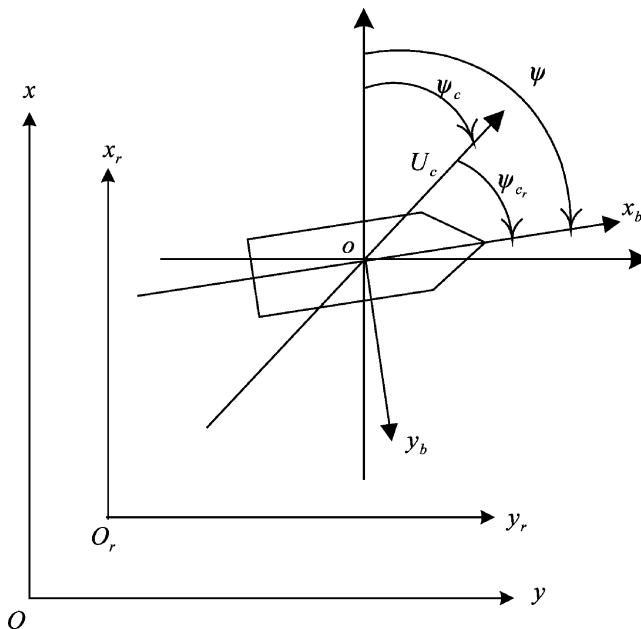


Fig. 2. Definition of coordinate systems and the speed and direction of current.

constant speed of current. Hydrodynamic force and moment acting on a ship are described easily with respect to the body-fixed frame, in which  $x_b$  and  $y_b$  axes are the directions of a ship's bow and starboard, respectively. All frames are right-handed orthogonal coordinate systems whose  $z$ -axes are positive downward. The body-fixed frame is assumed to coincide with the principal axes of a ship.

If roll motion can be neglected, and the force and moment from wave and wind are negligibly small compared to those by ambient water that may have constant velocity, the maneuvering motion in three degrees of freedom in the horizontal plane is represented by Newton's second law as follows,

$$\begin{aligned} m(\dot{u} - vr - x_{G_b}r^2) &= X_{HD,c} \\ m(\dot{v} + ur + x_{G_b}\dot{r}) &= Y_{HD,c} \\ I_z\dot{r} + mx_{G_b}(\dot{v} + ur) &= N_{HD,c} \end{aligned} \quad (1)$$

where subscript HD,c means the hydrodynamic force and moment, including the current effect.

Force and moment due to current can be included in the right hand side of Eq. (1) through simple modeling. Fossen (1994) and Hwang (1980) have modeled current effect by using the concept of relative velocity of a ship with respect to moving frame that moves at the constant speed of current. Hydrodynamic force and moment including its effect, therefore, can be expressed by the functions of relative motion variables instead of pure ones. Relative velocities can be written as

$$\begin{aligned} u_r &= u - U_c \cos\psi_{c_r} \\ v_r &= v + U_c \sin\psi_{c_r} \end{aligned} \quad (2)$$

Relative accelerations can be obtained by differentiating Eq. (2) with respect to time. Even though velocities have been changed into relative ones, the form of the left hand side of Eq. (1) remains unchanged.

Finally, the kinematic relations between the earth-fixed frame and the body-fixed frame are augmented to the system of equations of motion.

$$\begin{aligned} \dot{x} &= u \cos\psi - v \sin\psi \\ \dot{y} &= u \sin\psi + v \cos\psi \\ \dot{\psi} &= r \end{aligned} \quad (3)$$

## 2.2. Dynamic models of hydrodynamic force and current variables

Since accelerations are equivalent to hydrodynamic force and moment as shown in Eq. (1), the hydrodynamic components related to accelerations named as the components due to added mass cannot be estimated. We assumed that those components can be estimated to some extent, because added mass coefficients can be calculated by boundary element method or Inoue's empirical formula (Lewis, 1989).

Time-varying hydrodynamic force and moment represented by  $X$ ,  $Y$  and  $N$ , except the components due to added mass, can be modeled as the third-order

Gauss–Markov processes. These processes are widely used as black box models in signal processing when the characteristics of those time histories are a priori unknown and are smooth enough to represent quadratic curves in a short sampling interval. The speed and the direction of current are assumed to be constant.

$$\begin{aligned}\ddot{X} &= w_X(t) \\ \ddot{Y} &= w_Y(t) \\ \ddot{N} &= w_N(t)\end{aligned}\quad (4)$$

$$\begin{aligned}\dot{c}_x &= w_{c_x}(t) \\ \dot{c}_y &= w_{c_y}(t)\end{aligned}\quad (5)$$

where  $w$  represents the modeling errors associated with the assumptions of the dynamic models of hydrodynamic force and current variables.

### 2.3. State space model

State space model consists of a state equation and a measurement equation, which are represented with the state vector. Continuous-time state equation and discrete-time measurement equation are assumed in this study.

The components of state vector are the variables to be estimated, namely motion variables, hydrodynamic force and moment variables, and current variables. To estimate these variables by using state estimators such as a filter or a smoother, we need the dynamic models of state variables to be described or assumed. State equation represented by a vector form of the system of nonlinear first-order differential equations is composed of equations of motion (Eq. (1)), kinematic relations (Eq. (3)), and the dynamic models of hydrodynamic force and current variables (Eqs. (4) and (5)).

$$\dot{\underline{x}} = M^{-1}\underline{f}(\underline{x}) + \underline{w}(t) = M^{-1} \begin{bmatrix} m(v_r r + x_{G_b} r^2) + X \\ -m u_r r + Y \\ -m x_{G_b} u_r r + N \\ u_r \cos \psi - v_r \sin \psi \\ u_r \sin \psi + v_r \cos \psi \\ r \\ \dot{X} \\ \ddot{X} \\ 0 \\ \dot{Y} \\ \ddot{Y} \\ 0 \\ \dot{N} \\ \ddot{N} \\ 0 \\ 0 \\ 0 \end{bmatrix} + \begin{bmatrix} 0 \\ 0 \\ 0 \\ 0 \\ 0 \\ 0 \\ 0 \\ w_X(t) \\ 0 \\ 0 \\ w_Y(t) \\ 0 \\ 0 \\ w_N(t) \\ w_{C_x}(t) \\ w_{C_y}(t) \end{bmatrix} \quad (6)$$

where  $M$  is the inertia matrix, including the added mass coefficients, and  $\underline{w}(t)$  is assumed to be a white Gaussian noise process of mean zero and strength  $Q(t)$ . To estimate current variables along with motion variables and hydrodynamic force, we need to establish an observable state vector shown below,

$$\underline{x} = [u_r \quad v_r \quad r \quad x_r \quad y_r \quad \psi \quad \dot{X} \quad \dot{Y} \quad \ddot{X} \quad \ddot{Y} \quad \dot{N} \quad \ddot{N} \quad c_x \quad c_y]^T. \quad (7)$$

Actually, during sea trial, the number of measurements such as the position of a ship at DGPS antenna, its rate, heading angle, and relative surge velocity are fewer than those recorded in tests of airplanes or underwater vehicles. Heading angle and relative surge velocity are measured by gyrocompass and speed-log, respectively. If  $x$  and  $y$  are established as state variables instead of  $x_r$  and  $y_r$ , those cannot be estimated along with current variables because the measurements are not sufficient. Measurement equations are described as,

$$\underline{z} = \underline{h}(\underline{x}, t_k) + \underline{v}(t_k) = \begin{bmatrix} x_r + x_{D_b} \cos \psi - y_{D_b} \sin \psi + c_x t_k \\ y_r + x_{D_b} \sin \psi + y_{D_b} \cos \psi + c_y t_k \\ (u_r - y_{D_b} r) \cos \psi - (v_r + x_{D_b} r) \sin \psi + c_x \\ (u_r - y_{D_b} r) \sin \psi + (v_r + x_{D_b} r) \cos \psi + c_y \\ \psi \\ u_r - y_{S_b} r \end{bmatrix} + \underline{v}(t_k), \quad (8)$$

where  $(x_{D_b}, y_{D_b})$  and  $y_{S_b}$  are the known coordinates of DGPS antenna and speed-log with respect to the body-fixed frame respectively,  $t_k$  is discrete sampling time, which is zero at the start of maneuvering, and  $\underline{v}(t_k)$  is the measurement noise vector, which is assumed to be a white Gaussian noise sequence of mean zero and covariance  $R(t_k)$ .

### 3. Estimation of motion variables and hydrodynamic force and moment

#### 3.1. Extended Kalman filter and modified Bryson–Frazier smoother

State estimators for the state space model such as Eqs. (6) and (8) are classified as the predictor, the filter, and the smoother depending on the measurements data used to estimate states at an instant. Smoothed state is more efficient than predicted and filtered states, because the smoother can use all the measurements. Since smoothed state is derived from the filtered state, we will briefly summarize the EKF and the MBF smoother.

The EKF is widely used to estimate state variables of a nonlinear state space model. The algorithm is the same as that of the Kalman filter except that Jacobian matrices of the nonlinear equations with respect to state variables at an instant are used instead of linear system and measurement matrices. Since the properties and

the algorithm of the EKF are explained in many texts, we show only the final form of the filtered state vector and the error covariance matrix.

$$\begin{aligned}\hat{\underline{x}}(t_k|t_k) &= \hat{\underline{x}}(t_k|t_{k-1}) + K(t_k)\Delta\underline{z}(t_k|t_{k-1}) \\ P(t_k|t_k) &= [I - K(t_k)H(t_k)]P(t_k|t_{k-1})\end{aligned}\quad (9)$$

where  $\hat{\underline{x}}(t_k|t_k)$ ,  $P(t_k|t_k)$  and  $\hat{\underline{x}}(t_k|t_{k-1})$ ,  $P(t_k|t_{k-1})$  are the filtered state vector and the error covariance matrix and the single stage predicted state vector and the single stage error covariance matrix, respectively.  $K(t_k)$  and  $\Delta\underline{z}(t_k|t_{k-1})$  are the Kalman gain matrix calculated with  $P(t_k|t_{k-1})$  and an innovation process, which is the difference between measurements and the predicted, respectively.  $H(t_k)$  is the Jacobian matrix of Eq. (8) at  $t = t_k$ .  $\hat{\underline{x}}(t_k|t_{k-1})$  and  $P(t_k|t_{k-1})$  are propagated from  $\hat{\underline{x}}(t_{k-1}|t_{k-1})$  and  $P(t_{k-1}|t_{k-1})$ , which are the filtered values at the previous time step, by Eq. (6) and matrix Riccati differential equation.

There are three kinds of smoothers—fixed interval, fixed point, and fixed lag one—which can be used for different range of measurement. Among these, the fixed interval smoother is the most efficient state estimator, because it uses whole data obtained during measurement. Bierman (1973) modified the algorithm of the fixed interval smoother, first developed for a linear continuous system with linear discrete measurements by Bryson and Frazier. He defined the adjoint state vector  $\underline{\hat{z}}(t)$  and error covariance matrix  $\Lambda(t)$ . This vector and matrix are propagated in reverse time order by a linear system of first-order differential equations, represented by a Jacobian matrix of the state equation and matrix Riccati differential equation without a source term. They play a part as the state vector and the error covariance matrix in the EKF. The smoothed state vector and the error covariance matrix are calculated by using the filtered state vector and adjoint variables.

$$\begin{aligned}\hat{\underline{x}}(t_k|t_N) &= \hat{\underline{x}}(t_k|t_k) - P(t_k|t_k)\underline{\hat{z}}(t_k|t_k) \\ P(t_k|t_N) &= P(t_k|t_k) - P(t_k|t_k)\Lambda(t_k|t_k)P(t_k|t_k)\end{aligned}\quad (10)$$

where  $t_N$  is the final measurement time.

Fig. 3 shows the recursive algorithms of the EKF and the MBF smoother and their relationship.

### 3.2. Observability

Since the parameters to be estimated such as current variables are augmented to the state vector, the identifiability of the parameters are treated as the observability of the augmented state vector. If quasi-linear state estimators such as the EKF or the MBF smoother are used, the observability can be checked naturally by the linearized model described by the Jacobian matrix of state and measurement equations



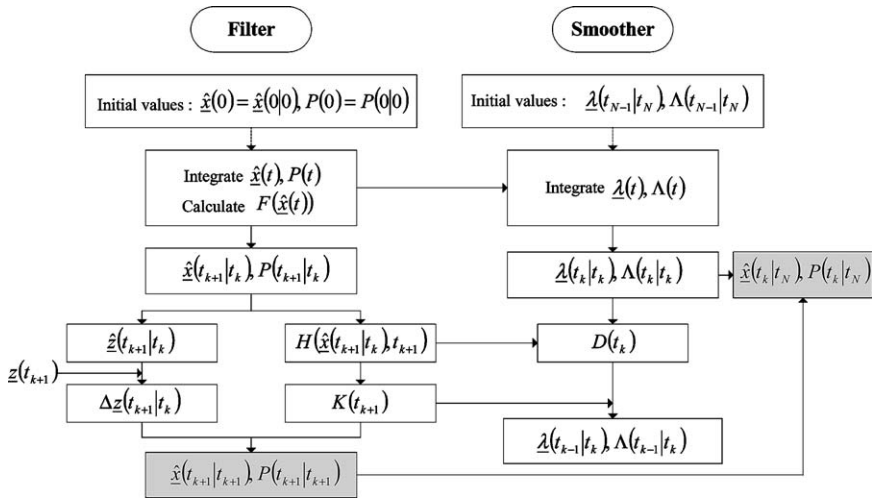


Fig. 3. Flowchart of EKF and MBF smoother.

at an instant. We will use the observability rank condition as the criterion of the observability. If the following observability matrix has rank  $n$ , which is the number of state variables, the system can be observable and then the parameters represented by the augmented state variables can be identified.

$$O(t_k) = \begin{bmatrix} H \\ HF \\ \vdots \\ HF^{n-1} \end{bmatrix}_{t=t_k}, \quad (11)$$

where  $F$  is the Jacobian matrix of the state equation at an instant.

In our problem, if we replace  $(x_r, y_r)$  with the absolute position vector  $(x, y)$  in Eq. (7), the rank of the observability matrix is  $n - 1$  and the observability is not guaranteed.

#### 4. Estimation of hydrodynamic coefficients

Given motion variables and the hydrodynamic force and moment estimated in the first step of EBM, we use regression analysis to identify the hydrodynamic coefficients in the model of hydrodynamic force as the second step. In addition,

specific characteristics of a ship maneuvering problem can be checked by correlation analysis.

#### 4.1. Regression model

Multiple linear regression models for the hydrodynamic force and moment are written as

$$\begin{aligned}\underline{X} &= H_X \underline{\theta}_X + \underline{\varepsilon}_X \\ \underline{Y} &= H_Y \underline{\theta}_Y + \underline{\varepsilon}_Y \\ \underline{N} &= H_N \underline{\theta}_N + \underline{\varepsilon}_N\end{aligned}\quad (12)$$

When there are  $p$  number of coefficients and  $N$  number of measurements,  $\underline{\theta}$  and  $H$  are the  $p \times 1$  hydrodynamic coefficient vector and the  $N \times p$  regressor matrix constructed by models of hydrodynamic force and moment, respectively.  $\underline{\varepsilon}$  is the error that cannot be explained by the regression model and should be assumed as a Gaussian random vector of zero mean.

Hydrodynamic coefficient vectors  $\underline{\theta}_X$ ,  $\underline{\theta}_Y$ , and  $\underline{\theta}_N$  are written as

$$\begin{aligned}\underline{\theta}_X &= [\eta'_{Cr} \quad \eta'_2 \quad \eta'_3 \quad X'_{vv} \quad X'_{vr} \quad X'_{rr} \quad X'_{vvr} \quad X'_{ee}]^T \\ \underline{\theta}_Y &= [Y'_0 \quad Y'_v \quad Y'_r \quad Y'_{vvv} \quad Y'_{vvr} \quad Y'_{vrr} \quad Y'_{rrr} \quad Y'_\delta \quad Y'_{eee}]^T, \\ \underline{\theta}_N &= [N'_0 \quad N'_v \quad N'_r \quad N'_{vvv} \quad N'_{vvr} \quad N'_{vrr} \quad N'_{rrr} \quad N'_\delta \quad N'_{eee}]^T\end{aligned}\quad (13)$$

where the symbols that are represented by  $X$ ,  $Y$ , and  $N$  for the forces and moment with subscripts of  $u$ ,  $v$ , and  $r$  for the motion variables are hydrodynamic coefficients, which are the partial derivatives of the corresponding force to motion variable at zero value. Superscript ( $'$ ) attached to each hydrodynamic coefficient means that the coefficient is constant and non-dimensional.

Regressor matrices are constructed by the modified Abkowitz's model suggested by Hwang (1980).

$$\begin{aligned}H_X &= \frac{\rho}{2} L^2 [\underline{h}_X(N), \underline{h}_X(N-1), \dots, \underline{h}_X(1)]^T \\ H_Y &= \frac{\rho}{2} L^2 [\underline{h}_Y(N), \underline{h}_Y(N-1), \dots, \underline{h}_Y(1)]^T \\ H_N &= L H_Y\end{aligned}\quad (14)$$

where

$$\underline{h}_X(k) = \begin{bmatrix} u_r(k)^2 \\ Lnu_r(k) \\ L^2n^2 \\ v_r(k)^2 \\ Lv_r(k)r(k) \\ L^2r(k)^2 \\ L^2 \frac{v_r(k)^2r(k)^2}{U_r(k)^2} \\ c(k)^2e(k)^2 \end{bmatrix},$$

$$\underline{h}_Y(k) = \begin{bmatrix} \left(\frac{u_{A\infty}(k)}{2}\right)^2 \\ U_r(k)v_r(k) \\ LU_r(k)r(k) \\ \frac{v_r(k)^3}{U_r(k)} \\ L \frac{v_r(k)^2r(k)}{U_r(k)} \\ L^2 \frac{v_r(k)r(k)^2}{U_r(k)} \\ L^3 \frac{r(k)^3}{U_r(k)} \\ [c(k) - c_0] \left[ \frac{L}{2}r(k) - v_r(k) \right] + c(k)^2\delta(k) \\ c(k)^2e(k)^3 \end{bmatrix}, \quad (15)$$

where  $k = 1, 2, \dots, N$ .

#### 4.2. Correlation analysis

Correlation of mutual regressors in the multiple linear regression model (Eq. (12)) shows the specific properties of experiments in the viewpoint of regression analysis. A correlation matrix can be obtained by unit-length scaling of each column of the regressor matrix  $H$ . If unit-length scaling and centering are carried out, intercepts have to be included in the original regression model. Since intercepts have no physical meaning in the models of hydrodynamic force and moment, centering is not performed in this study. If the scaled regressor matrix is  $W$ ,

correlation matrix becomes  $W^T W$ , of which the  $(i,j)$  component is the correlation coefficient between the  $i$ th and the  $j$ th regressors.

### 4.3. Hydrodynamic coefficients

If one of the original regression models (Eq. (12)) is transformed through unit-length scaling as follows,

$$\underline{y} = W\underline{\beta} + \underline{\varepsilon}, \quad (16)$$

$\hat{\underline{\beta}}$  can be obtained by a regression method, where the symbol ‘ $\wedge$ ’ means that the value is not the true but an estimated random one. The relationship between  $\hat{\underline{\beta}}$  and the original coefficient vector  $\hat{\underline{\theta}}$  is as follows,

$$\hat{\theta}_j = \hat{\beta}_j \sqrt{\frac{S_{yy}}{S_{jj}}}, \quad j = 1, 2, \dots, p, \quad (17)$$

where  $S_{yy}$  and  $S_{jj}$  are the sums of squares of observation and the  $j$ th regressor, respectively.

If multicollinearity exists in the regression model, the variance of estimated coefficient is very large. To reduce the variance even if the bias is allowed, ridge regression method (Montgomery and Peck, 1982) is used.

$$\hat{\underline{b}} = (W^T W + kI)^{-1} W^T \underline{y}, \quad (18)$$

where  $k$  is called the biasing parameter, which can be automatically adjusted by Hoerl's iterative estimation procedure (Hoerl and Kennard, 1970). In our study, ridge regression method is employed because it is slightly more stable, although it did not improve the performance of identification considerably for strong multicollinearity.

## 5. Results and discussion

### 5.1. Simulation

To validate the developed algorithm, we applied the algorithm to identify hydrodynamic coefficients of ESSO OSAKA (Hwang, 1980). 35° turning circle test and 20°–20° zig-zag test were simulated to generate a set of measurement data, of which standard deviations are assumed as follows,

$$\begin{aligned} \sigma_{x_G} = \sigma_{y_G} = 10 \text{ m}, \quad \sigma_{\dot{x}_G} = \sigma_{\dot{y}_G} = 0.01 \text{ m/s}, \quad \sigma_{\psi} = 0.0008^\circ, \\ \sigma_{u_{rS}} = 0.01 \text{ m/s}. \end{aligned} \quad (19)$$

Also 10° PRBS command rudder test was simulated to validate the estimated hydrodynamic model. The speed and the direction of current were assumed to be 2 knots and 45°, respectively.

### 5.1.1. Estimation of motion variables, hydrodynamic force, and current variables

Fig. 4 illustrates the results of estimated motion variables, hydrodynamic force and moment, and  $x$ ,  $y$  components of current speed with respect to the earth-fixed frame in a  $20^\circ$ – $20^\circ$  zig-zag test. Since the accuracy of initial state values influence the performance of estimation at initial stage, current variables were obtained from the first estimation, and then state estimation was carried out again with initial velocities corrected by the previously estimated current variables.

Smoothed motion variables such as sway velocity and heading angle rate, which are not measured, agree well with true ones. Except at the time when rudder angle is changed, smoothed hydrodynamic force and moment agree with the true values, as well. Filtered state estimates are improved by the MBF smoother.

### 5.1.2. Identification of hydrodynamic coefficients

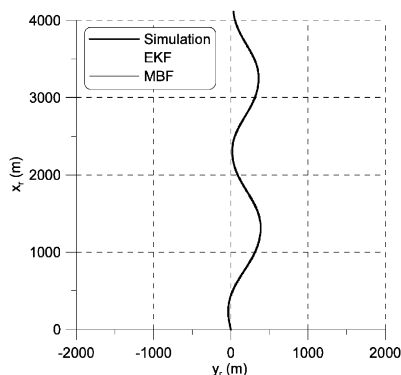
Hydrodynamic coefficients are identified by using the estimated motion variables, hydrodynamic force and moment of  $35^\circ$  starboard and port turning circle tests and  $20^\circ$ – $20^\circ$  zig-zag test. The results of those tests are collected and treated as one set of experiment in regression analysis.

Tables 1 and 2 show the correlation coefficients of mutual regressors and those between each regressor and responses in surge and sway regression models of hydrodynamic force. The regressors in the model of yaw hydrodynamic moment is the same as the ones of sway hydrodynamic force, except dimensions of those variables (Eq. (14)).

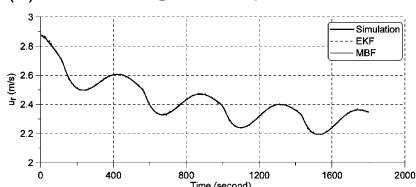
Nonlinear regressors with respect to motion variables and sway velocity and heading angle rate, highly correlate as shown in Tables 1 and 2. Whereas nonlinear coefficients can be regarded as simple correction terms in the model, linear coefficients such as  $Y'_v$ ,  $N'_v$ ,  $Y'_r$ , and  $N'_r$ , named as stability coefficients, have important physical meanings. The higher correlation of regressors is, or the stronger multicollinearity exists, the more difficult it is to identify regression coefficients separately. The multicollinearity is the same phenomenon as the simultaneous drift first suggested by Hwang (1980). Since a conventional ship is maneuvered by a single control device, i.e. rudder, the drift angle takes place inevitably. For this reason, the identification of hydrodynamic coefficients has to be improved in a sea trial scenario; therefore, we will propose an input scenario to mitigate the effect later.

Table 3 shows the true and identified hydrodynamic coefficients by ridge regression method. Condition numbers of  $W^T W$  ( $\kappa$ ), coefficients of multiple determination ( $R$ ), and Mallows'  $C_p$  statistics are shown in Table 4 for the adequacies of regression models. The bigger  $\kappa$  is, the stronger multicollinearity exists in regression model. And  $C_p$  converges ideally to  $p$ , which are, 8, 9, and 9 in surge, sway, and yaw equations, respectively. The number in parenthesis means the power of ten for notational convenience.

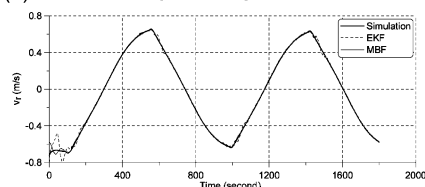
The true nonlinear coefficients differ considerably from the identified ones due to multicollinearity. Since sway velocity and heading angle rate are nearly linearly related, even linear coefficients hardly coincide with true ones, separately. If the

(a)  $x, y$  trajectory

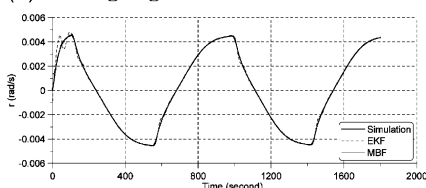
(b) Relative surge velocity



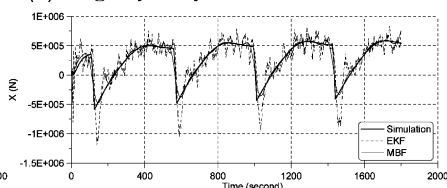
(c) Relative sway velocity



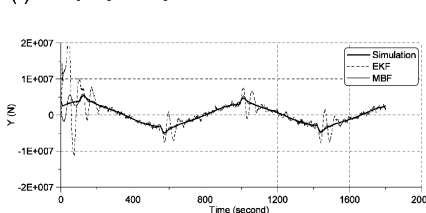
(d) Heading angle rate



(e) Surge hydrodynamic force



(f) Sway hydrodynamic force



(g) Yaw hydrodynamic moment

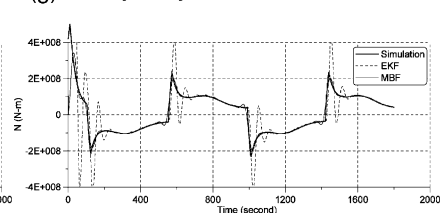
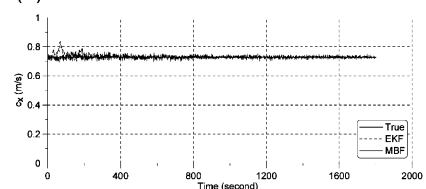
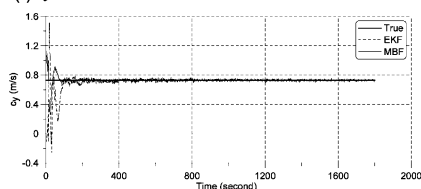
(h)  $x$  component of current speed(i)  $y$  component of current speed

Fig. 4. Estimated motion variables, hydrodynamic force and moment, and current variables for ESSO OSAKA in case of  $20^\circ$ – $20^\circ$  zig-zag test.



Table 3  
True and identified hydrodynamic coefficients in the regression models for ESSO OSAKA

Coefficients	True	Estimated	Coefficients	True	Estimated	Coefficients	True	Estimated
$\eta'_{C_R}$	-6.98 (-4)	-1.10 (-4)	$Y'_0$	1.90 (-6)	-3.13 (-5)	$N'_0$	-2.25 (-6)	-1.53 (-5)
$\eta'_2$	-9.65 (-6)	-2.45 (-5)	$Y'_v$	-2.83 (-2)	-5.99 (-2)	$N'_v$	-1.09 (-2)	-1.39 (-2)
$\eta'_3$	3.83 (-7)	4.53 (-7)	$Y'_r$	3.91 (-3)	-9.25 (-3)	$N'_r$	-5.00 (-3)	-6.34 (-3)
$X'_{vv}$	-6.00 (-3)	-1.28 (-3)	$Y'_{vv}$	-1.06 (-1)	3.56 (0)	$N'_{vv}$	3.16 (-3)	5.66 (-1)
$X'_{vr}$	6.36 (-3)	9.49 (-3)	$Y'_{vvr}$	-1.15 (-2)	3.97 (0)	$N'_{vvr}$	-1.18 (-2)	6.25 (-1)
$X'_{rr}$	5.15 (-3)	6.28 (-3)	$Y'_{vrr}$	-4.13 (-2)	1.43 (0)	$N'_{vrr}$	9.05 (-3)	2.51 (-1)
$X'_{vrr}$	-7.15 (-3)	-1.07 (-2)	$Y'_{rrr}$	-5.19 (-2)	1.78 (-1)	$N'_{rrr}$	-1.24 (-3)	2.95 (-1)
$X'_{ee}$	-2.49 (-3)	-2.26 (-3)	$Y'_{s}$	5.08 (-3)	3.67 (-3)	$N'_s$	-2.42 (-3)	-2.55 (-3)
			$Y'_{eee}$	-1.85 (-3)	4.42 (-3)	$N'_{eee}$	9.70 (-4)	2.24 (-3)



Table 4

Parameters for model adequacies to the regression models for ESSO OSAKA

Mode	$\kappa$	$R$	$C_p$
Surge	3.7220 (4)	0.9890	8.0545
Sway	2.8251 (6)	0.9823	9.0536
Yaw	2.8166 (6)	0.9198	9.0808

and moment acting on a ship due to consistent combined coefficients in Eq. (21), even though each hydrodynamic coefficient cannot be determined separately.

### 5.1.3. Validation of estimated hydrodynamic model through $10^\circ$ PRBS command rudder test

To validate estimated regression model's time history of rudder deflection angle of PRBS type commanded every 400 second with  $\pm 10^\circ$  is generated as depicted in Fig. 5.

Fig. 6 shows motion variables and hydrodynamic force and moment simulated by estimated regression models in comparison with true ones. There are some errors in  $x, y$  trajectory and heading angle, because those position values and errors are integrated together. The other motion variables and the hydrodynamic force and moment agree with true values on the whole.

### 5.1.4. Input design

To enhance the estimation performance in the scaled regression model such as Eq. (16), we determined the input scenario, so that  $|W^T W|$  was maximized within the constraint of ship dynamics, which is the D-optimality criterion in experimental design. Since the columns of  $W$  is the dynamic response of a ship to rudder deflection angle,  $|W^T W|$  may be a function of the maximum command rudder angle and its period of PRBS which is known to be the optimal input in case of moving average dynamic model (Fig. 7). Under the assumption that the speed of current can be controlled, Fig. 8 shows the variation of  $|W^T W|$  as a function of the speed of current.

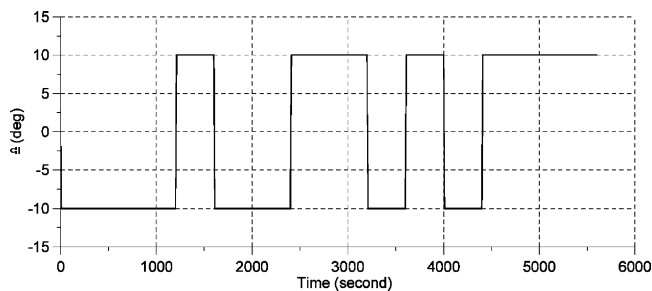
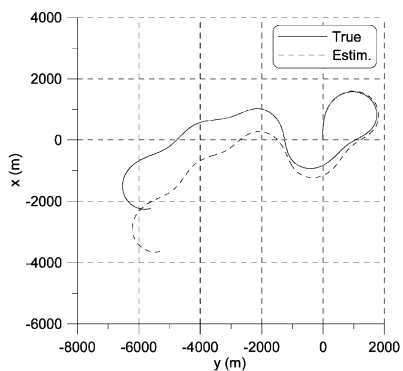
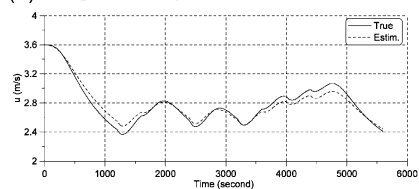


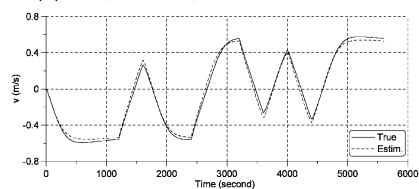
Fig. 5. Time history of rudder deflection angle for  $\pm 10^\circ$  PRBS rudder command.

(a)  $x, y$  trajectory

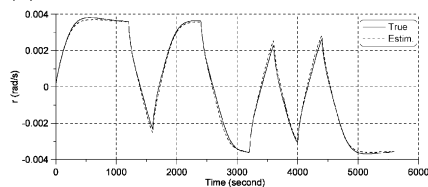
(b) Surge velocity



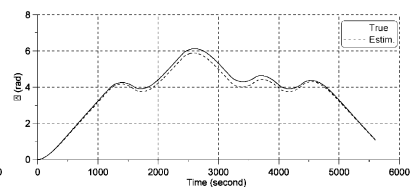
(c) Sway velocity



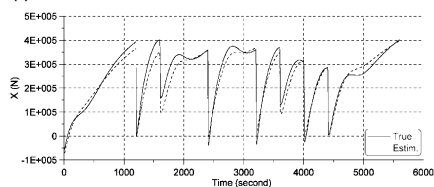
(d) Heading angle rate



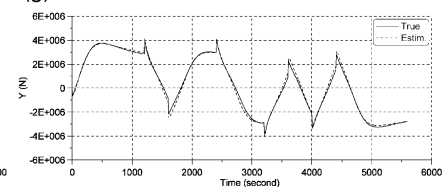
(e) Heading angle



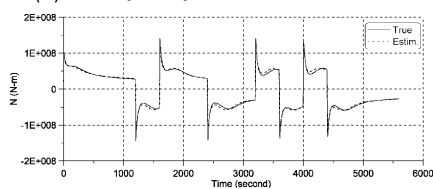
(f) Surge hydrodynamic force



(g) Sway hydrodynamic force



(h) Yaw hydrodynamic moment

Fig. 6. Motion variables and hydrodynamic force and moment for  $\pm 10^\circ$  PRBS rudder command.

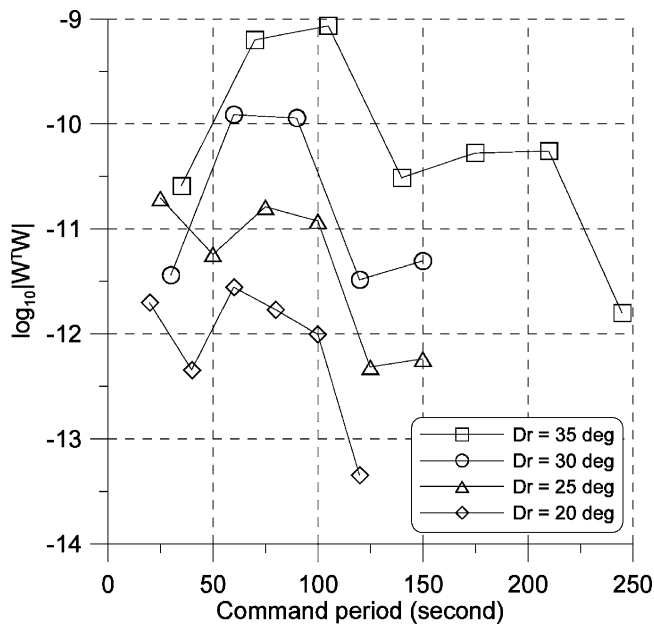


Fig. 7. D-optimality criterion depending on different command rudder angle and period of PRBS input.

In Fig. 7, the case in which the command rudder angle and the period of PRBS input are  $35^\circ$  and 105 seconds, respectively, is the most optimal than other cases. When the command period is too short, a ship cannot be followed on the rudder deflection, because the ship responds slowly to an external disturbance. On the other hand, if the period is too long, the motion of a ship remains in steady state which is not sufficiently rich in view of identification. If the speed of current can be controlled in the case that a model ship maneuvers in a square tank equipped with current generator, a better input scenario can be obtained, as shown in Fig. 8.

Table 5 shows the identified hydrodynamic coefficients obtained using the optimal PRBS rudder input scenario without considering the effect of current. Linear coefficients and even nonlinear coefficients converge to the true ones.

## 5.2. Sea trials

The algorithm was also applied to the real sea trial data of 113K tanker. Data from  $35^\circ$  turning circle test and  $20^\circ$ – $20^\circ$  zig-zag test were used to obtain regression models in the same manner depicted in Section 5.1. The simulation result of  $10^\circ$ – $10^\circ$  zig-zag test by the estimated regression models was compared with the sea trial data.

### 5.2.1. Estimation of motion variables, hydrodynamic force, and current variables

Fig. 9 depicts estimated motion variables, hydrodynamic force and moment, and current variables for  $20^\circ$ – $20^\circ$  zig-zag test. Estimated unmeasured motion variables

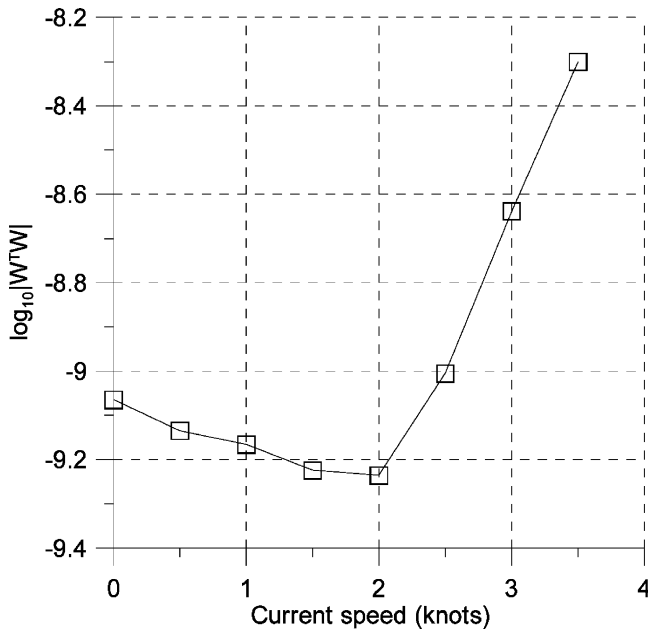


Fig. 8. D-optimality criterion depending on different current speed when the command rudder angle and period of PRBS input are  $35^\circ$  and 105 seconds, respectively.

such as relative sway velocity and heading angle rate, and hydrodynamic force followed similar tendency as shown in Fig. 4. The decrease of the sway velocity on the initial interval shown in Fig. 9(c) results from the positive initial sway velocity due to current speed. The speed and the direction of current was converged well.

#### 5.2.2. Identification of hydrodynamic coefficients

Tables 6–9 list the correlation coefficients, identified hydrodynamic coefficients and the parameters for the adequacies of the regression models, respectively. Notice that the sign of rudder deflection angle for 113K tanker is the opposite for ESSO OSAKA.

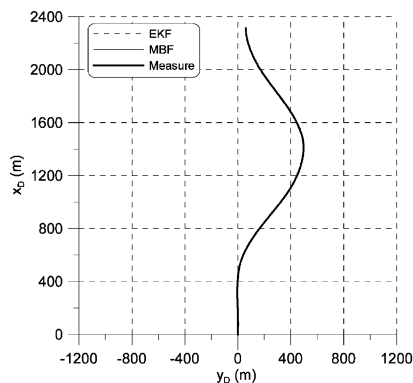
Tables 6 and 7 show that correlation coefficients have similar tendencies as those in the case of ESSO OSAKA. Since  $N'_r$  in Table 9 should not be negative and  $R$  of yaw regression model is very low, the model should be modified. A complex functions of motion variables and rudder deflection angle (Eq. (15)), the form of moment component generated by the rudder is modified simply as follows,

$$\begin{aligned} & \frac{\rho}{2} L^3 \left[ N'_\delta \left\{ (c - c_0) \left( \frac{L}{2} r - v_r \right) + c^2 \delta \right\} + N'_{eee} c^2 e^3 \right] \\ \Rightarrow & \frac{\rho}{2} L^3 (N'_\delta U_r^2 \delta + N'_{eee} U_r^2 e^3). \end{aligned} \quad (22)$$

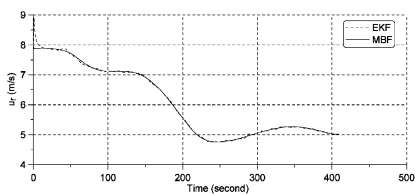
The hydrodynamic coefficients in the modified model of yaw hydrodynamic moment are shown in Table 10. When the model was modified,  $R$  became 0.8901,

Table 5  
True and identified hydrodynamic coefficients in the regression models for ESSO OSAKA when the sub-optimal PRBS rudder input scenario is applied

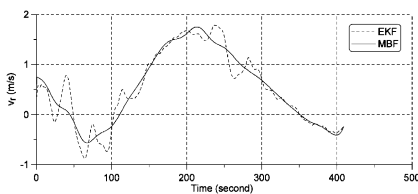
Coefficients	True	Estimated	Coefficients	True	Estimated	Coefficients	True	Estimated
$\eta'_{C_R}$	-6.98 (-4)	-3.85 (-4)	$Y'_0$	1.90 (-6)	-1.48 (-5)	$N'_0$	-2.25 (-6)	-3.17 (-6)
$\eta'_2$	-9.65 (-6)	-1.25 (-5)	$Y'_i$	-2.83 (-2)	-2.44 (-2)	$N'_i$	-1.09 (-2)	-1.08 (-2)
$\eta'_3$	3.83 (-7)	3.07 (-7)	$Y'_r$	3.91 (-3)	6.17 (-3)	$N'_r$	-5.00 (-3)	-4.81 (-3)
$X'_{vv}$	-6.00 (-3)	-1.63 (-2)	$Y'_{vvv}$	-1.06 (-1)	-1.29 (-1)	$N'_{vvv}$	3.16 (-3)	-3.80 (-4)
$X'_{vr}$	6.36 (-3)	3.87 (-3)	$Y'_{vvr}$	-1.15 (-2)	-3.27 (-2)	$N'_{vvr}$	-1.18 (-2)	-1.29 (-2)
$X'_{rr}$	5.15 (-3)	5.93 (-3)	$Y'_{vrr}$	-4.13 (-2)	-5.06 (-2)	$N'_{vrr}$	9.05 (-3)	9.51 (-3)
$X'_{vrrr}$	-7.15 (-3)	-2.43 (-3)	$Y'_{rrr}$	-5.19 (-2)	-6.11 (-3)	$N'_{rrr}$	-1.24 (-3)	-9.88 (-4)
$X'_{ee}$	-2.49 (-3)	-1.84 (-3)	$Y'_\delta$	5.08 (-3)	5.67 (-3)	$N'_\delta$	-2.42 (-3)	-2.32 (-3)
			$Y'_{eee}$	-1.85 (-3)	-2.56 (-3)	$N'_{eee}$	9.70 (-4)	8.00 (-4)

(a)  $x, y$  trajectory of DGPS antenna

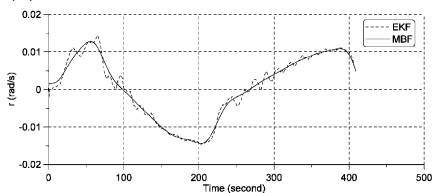
(b) Relative surge velocity



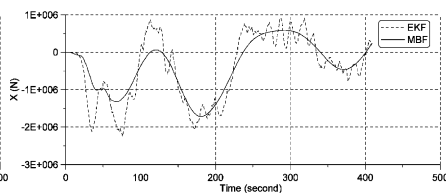
(c) Relative sway velocity



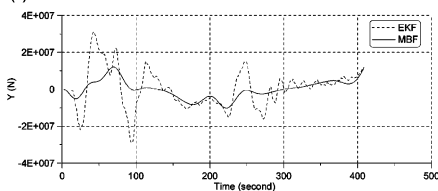
(d) Heading angle rate



(e) Surge hydrodynamic force



(f) Sway hydrodynamic force



(g) Yaw hydrodynamic moment

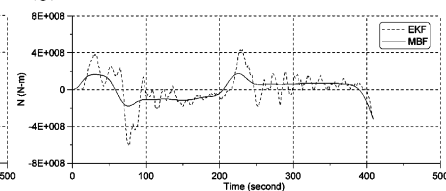
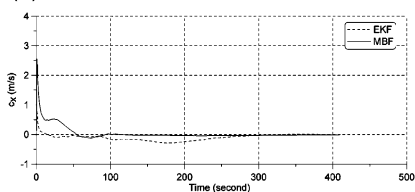
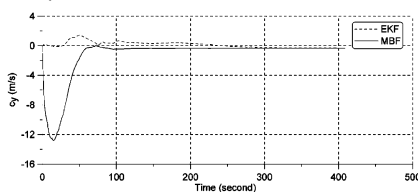
(h)  $x$  component of current speed(i)  $y$  component of current speed

Fig. 9. Estimated motion variables, hydrodynamic force and moment, and current variables for 113K tanker in case of  $20^\circ$ – $20^\circ$  zig–zag test.

Table 6

Correlation coefficients of surge regression model for 113K tanker

	$\eta'_{C_R}$	$\eta'_2$	$\eta'_3$	$X'_{vv}$	$X'_{vr}$	$X'_{rr}$	$X'_{vrr}$	$X'_{ee}$
$\eta'_{C_R}$	1.00	0.97	0.79	0.53	−0.51	0.61	0.35	0.53
$\eta'_2$		1.00	0.91	0.67	−0.65	0.73	0.51	0.69
$\eta'_3$			1.00	0.74	−0.74	0.81	0.70	0.86
$X'_{vv}$				1.00	−0.94	0.85	0.86	0.78
$X'_{vr}$					1.00	−0.96	−0.92	−0.89
$X'_{rr}$						1.00	0.86	0.93
$X'_{vrr}$							1.00	0.89
$X'_{ee}$								1.00

Table 7

Correlation coefficients of sway regression model for 113K tanker

	$Y'_0$	$Y'_v$	$Y'_r$	$Y'_{vv}$	$Y'_{vr}$	$Y'_{rr}$	$Y'_{vrr}$	$Y'_\delta$	$Y'_{eee}$
$Y'_0$	1.00	0.14	0.01	0.17	−0.11	0.10	−0.10	0.01	−0.03
$Y'_v$		1.00	−0.84	0.86	−0.82	0.81	−0.78	−0.57	−0.76
$Y'_r$			1.00	−0.70	0.77	−0.79	0.83	0.76	0.82
$Y'_{vv}$				1.00	−0.96	0.90	−0.82	−0.59	−0.78
$Y'_{vr}$					1.00	−0.98	0.92	0.74	0.89
$Y'_{rr}$						1.00	−0.98	−0.80	−0.95
$Y'_{vrr}$							1.00	0.86	0.98
$Y'_\delta$								1.00	0.92
$Y'_{eee}$									1.00

and the regression model provided considerably better fit compared with that of the previous model.

### 5.2.3. Validation of estimated hydrodynamic model through $10^\circ$ – $10^\circ$ zig–zag test

Fig. 10 shows the motion variables obtained by simulation with the identified coefficients as well as the measured variables of the  $10^\circ$ – $10^\circ$  zig–zag test. The speed and the direction of current were 0.66 m/s and  $-110.4^\circ$ , respectively, which were estimated by EBM.

There is a measurement error in the surge velocity relative to water during initial stage as shown in Fig. 10(e). When a ship begins to maneuver, the surge velocity might decrease in general, but on the other hand, the measured is rather shown to increase during that stage. Even though there are some errors in the time histories of trajectory and heading angle obtained by integrating the velocities, the magnitudes of deviation range and the overshoot heading angle calculated by simulation with estimated regression model agree well with those from the measured data. If the surge velocity can be measured more precisely, more consistent results can be expected.

Table 8  
Identified hydrodynamic coefficients in the regression models for 113K tanker

Coefficients	Value	Coefficients	Value	Coefficients	Value
$\eta'_{C_R}$	-4.30 (-4)	$Y'_0$	8.34 (-4)	$N'_0$	-2.37 (-4)
$\eta'_2$	-1.95 (-5)	$Y'_v$	-5.22 (-3)	$N'_v$	1.30 (-3)
$\eta'_3$	4.74 (-7)	$Y'_r$	6.47 (-3)	$N'_r$	1.33 (-3)
$X'_{v_v}$	-8.18 (-4)	$Y'_{vv}$	1.05 (-1)	$N'_{vv}$	-8.12 (-3)
$X'_{vr}$	3.43 (-3)	$Y'_{vvr}$	3.10 (-1)	$N'_{vvr}$	-4.05 (-2)
$X'_{rr}$	-5.51 (-3)	$Y'_{vrr}$	1.92 (-1)	$N'_{vrr}$	-2.58 (-2)
$X'_{vrr}$	5.77 (-3)	$Y'_{rrr}$	4.19 (-2)	$N'_{rrr}$	-8.18 (-3)
$X'_{ee}$	-1.83 (-4)	$Y'_s$	-3.73 (-3)	$N'_s$	4.09 (-4)
		$Y'_{eee}$	3.22 (-3)	$N'_{eee}$	3.22 (-4)



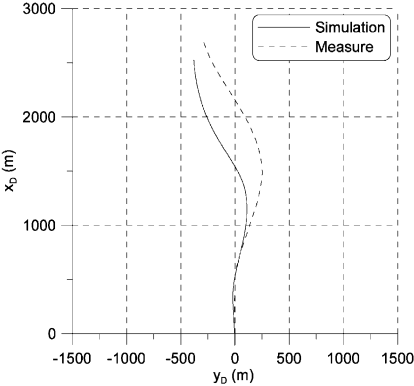
Table 9  
Parameters for model adequacies to the regression models for 113K tanker

Mode	$\kappa$	$R$	$C_p$
Surge	6.6779 (3)	0.9656	8.0629
Sway	1.6106 (4)	0.9613	9.3241
Yaw	1.5646 (4)	0.7478	9.4989

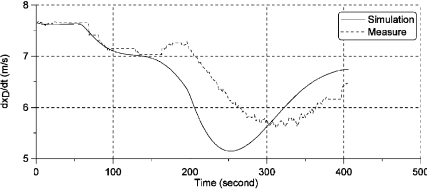
Table 10  
Hydrodynamic coefficients in the modified yaw regression model for 113K tanker

$N'_0$	$N'_v$	$N'_r$	$N'_{vvv}$	$N'_{vvr}$	$N'_{vrr}$	$N'_{rrr}$	$N'_\delta$	$N'_{eee}$
-2.97 (-5)	-7.79 (-4)	-6.89 (-4)	1.62 (-2)	1.36 (-2)	7.02 (-3)	1.07 (-3)	1.50 (-3)	-1.33 (-5)

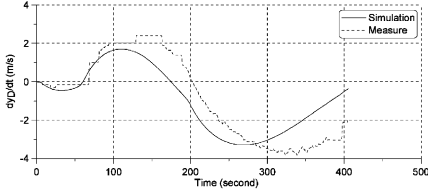
(a)  $x, y$  trajectory of DGPS antenna



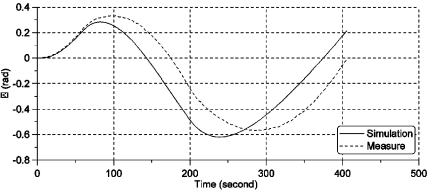
(b)  $\dot{x}_D$



(c)  $\dot{y}_D$



(d) Heading angle



(e) Surge velocity

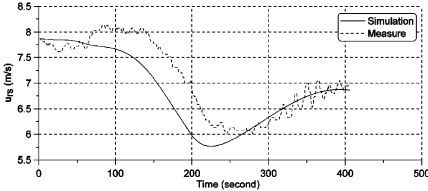


Fig. 10. Comparison of simulation results through estimated hydrodynamic coefficients with those of real  $10^\circ-10^\circ$  zig-zag test.

## 6. Conclusions

EBM technique was first applied to a ship maneuvering problem. The number of measurements are insufficient compared to an airplane and ship's dynamics is slow. Unmeasured motion variables and hydrodynamic force and moment can be successfully estimated along with the speed and the direction of current after setting up the observable state space model. Hydrodynamic coefficients are difficult to be identified separately by the standard maneuvering trials such as turning circle test and zig-zag test because of the strong multicollinearity in the regression model; therefore, a more sufficient rich input scenario as sub-optimal one has been suggested. We validated the developed algorithm by applying it to the data obtained from sea trials.

## References

- Abkowitz, M.A., 1980. Measurement of hydrodynamic characteristics from ship maneuvering trials by system identification. *SNAME Trans.* 88.
- Bierman, G.J., 1973. Fixed interval smoothing with discrete measurements. *Int. J. Control* 18 (1), 65–75.
- Crane, C.L., 1979. Maneuvering trials of a 278000-DWT tanker in shallow and deep waters. *SNAME Trans.* 87, 251–283.
- Fossen, T.I., 1994. *Guidance and Control of Ocean Vehicles*. John Wiley & Sons.
- Hoerl, A.E., Kennard, R.W., 1970. Ridge regression: biased estimation for nonorthogonal problems. *Technometrics* 12 (1), 55–67.
- Hoff, J.C., 1995. *Aircraft Parameter Estimation by Estimation-Before-Modelling Technique*. Ph.D. Thesis, Cranfield University.
- Hoff, J.C., Cook, M.V., 1996. Aircraft parameter identification using an estimation-before-modelling. *Aeronaut. J.*, 259–268.
- Hwang, W., 1980. *Application of System Identification to Ship Maneuvering*. Ph.D. Thesis, Massachusetts Institute of Technology.
- Källström, C.G., 1979. *Identification and Adaptive Control Applied to Ship Steering*. Ph.D. Thesis, Lund Institute of Technology.
- Kobayashi, E., Kagemoto, H., Furukawa, Y., 1995. Research on ship manoeuvrability and its application to ship design. Chapter 2: mathematical models of manoeuvring motions. In: *The 12th Marine Dynamic Symposium*, pp. 23–90.
- Lewis, E.V., 1989. Principles of naval architecture. Motions in Waves and Controllability. second ed. In: *SNAME*, vol. III, pp. 217–221.
- Liu, G., 1988. *Measurement of Ship Resistance Coefficient from Simple Trials During a Regular Voyage*. Ph.D. Thesis, Massachusetts Institute of Technology.
- Montgomery, D.C., Peck, E.A., 1982. *Introduction to Linear Regression Analysis*. John Wiley & Sons.
- Sri-Jayantha, M., Stengel, R.F., 1988. Determination of nonlinear aerodynamic coefficients using the estimation-before-modeling method. *J. Aircraft* 25 (9), 796–804.
- Yoon, H.K., Rhee, K.P., 2001. Estimation of external forces and current variables in sea trial by using the estimation-before-modeling method. *J. Soc. Naval Archit. Korea* 38 (4), 30–38.